sustainability

MDPI

Article

Experimental Study on Electrode Method for Electrical Resistivity Survey to Detect Cavities under Road Pavements

Chang-Seon Park [1,2], Jin-Hoon Jeong [3], Hae-Won Park [3] and Kyoungchul Kim [4,*]

[1] Department of Civil Engineering, Inha University, 100 Inha-ro, Nam-gu, Incheon 22212, Korea; cseon90@kistec.or.kr

[2] Currently Bridge & Tunnel Safety Section, Safety Division, Korea Infrastructure Safety & Technology Corporation, 16 123 Sadeul-ro, Gyeongsangnam-do, Jinju 52852, Korea

[3] Department of Civil Engineering, Inha University, 100 Inha-ro, Nam-gu, Incheon 22212, Korea; jhj@inha.ac.kr (J.-H.J.); spro374@naver.com (H.-W.P.)

[4] R&D Center, KOLON Global Corporation, 32 Songdogwahak-ro, Yeonsu-gu, Incheon 21984, Korea

* Correspondence: kckim@kolon.com; Tel.: +82-10-8898-4676

Received: 16 October 2017; Accepted: 10 December 2017; Published: 13 December 2017

Abstract: There are two types of electrode methods for electrical resistivity survey (ERS): the pole electrode method (PEM) and flat electrode method (FEM). During the past few decades, most studies were conducted by using PEM for various purposes while only a few were conducted by using FEM. Laboratory and field experiments were performed in this study to investigate the advantage of FEM in detecting cavities under pavements. In the laboratory experiment, the results of PEM and FEM were compared graphically and statistically. A significant difference between the results of PEM and FEM was observed for concrete at an age of seven days, while there was no significant difference in the results for soil materials. Electrical resistivity could not be obtained from asphalt because it is an insulator. In a field experiment, four different cases were simulated: field ground with/without cavity and concrete pavement with/without cavity. The results of PEM and FEM for these cases were compared using 2D electrical resistivity contour images. It was observed that the distribution of electrical resistivity obtained using FEM was wider than that using PEM. Moreover, the locations of the cavities artificially made in the ground and under the pavement were accurately detected using both PEM and FEM.

Keywords: electrical resistivity; pole electrode method; flat electrode method; cavity; pavement

1. Introduction

Electrical resistivity survey (ERS) is a time- and cost-effective non-destructive method of producing the shape and location image of an object. It can be used in various applications such as in detecting underground water and cavities, faults, and cracks [1–7]. Generally, ERS is performed by installing an electrode made of a conductive material. As shown in Figure 1a, the pole electrode method (PEM) performed by inserting a pole conductor into an object has been commonly used for ERS [3,8,9]. Since pavement collapse frequently occurs due to cavities generated under pavements, various nondestructive survey methods have been widely used in the preobservation of status under pavements [2,10–12]. However, it is difficult to apply ERS to pavements using PEM as the pole conductor may seriously damage the pavement during insertion. To overcome the disadvantage of PEM, the flat electrode method (FEM), which involves contacting a flat conductor to an object as shown in Figure 1b, is recommended when applying ERS to pavements [3,5,8,9]. Moreover, the application of the FEM can prevent the secondary damage occurred by pavement surface damage and preserve the sustainability of the infrastructure lost due to pavement collapse disasters.

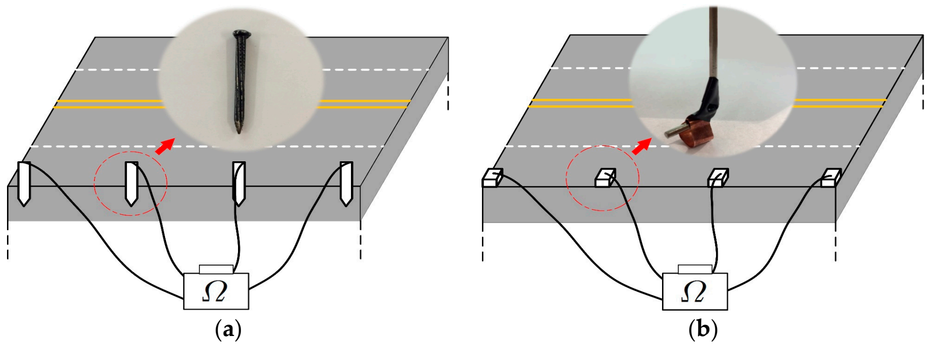

Figure 1. Electrode installation methods for electrical resistivity survey: (**a**) PEM; (**b**) FEM.

During the past few decades, most of the studies used PEM for detecting cavities under pavements under various conditions, while only a few used FEM [4–6,13–16]. Park et al. [4] examined the applicability of three-dimensional ERS to detect the cavities under a ground subsidence area by comparing the results of borehole tests performed at field experiment sites. As the cavities were mostly filled with water and clays in the test sites in accordance with the results of the borehole test, a low electrical resistivity was observed at the locations. Thus, it was shown that ERS was effective in detecting cavities underground subsidence areas.

Farooq et al. [5] examined the electrical resistivity of Portland cement mortar specimens with various water-cement (w/c) ratios by using PEM for evaluating cement mortar grouted locations. A significant correlation between the electrical resistivity and w/c was observed. Although the electrical resistivity was proportional to the curing time of the mortar, it was inversely proportional to w/c. Thus, it was shown that ERS is applicable to cement mortar grouted locations. Gambetta et al. [6] observed the geophysical response of a shallow cave by using PEM. The results showed clear geophysical responses of large cave passages by high electrical resistivity. Moreover, it was confirmed that locations of voids were precisely detected using ERS even under complex environments.

Recently, Cai et al. [14] developed an empirical equation based on the correlation between electrical resistivity and reactive magnesia content to predict the resistivity of carbonated soils.

The electrical resistivity computed using that equation in accordance with t and w_0/c was compared with the experimentally obtained electrical resistivity. Reasonable degrees of correlation were found between the model and the experimental results.

Generally, as concrete and asphalt pavements have high electrical resistance, the contact resistance between the electrode and pavement surface is the most important factor in an ERS [5,9]. In particular, FEM, which has a wider contact area, is more influenced by contact resistance than PEM [3,8]. In this study, laboratory and field experiments were performed to investigate the advantage of FEM in detecting cavities under pavements. The correlation between electrical properties and constituents of pavement layers were obtained from the laboratory experiments. The applicability of FEM for detecting cavities was investigated by applying the method to the field site where the concrete pavement and cavity were simulated artificially.

2. Theoretical Background of ERS

2.1. Outline of ERS

The amount of flowing electrical current is determined when a constant voltage is applied to the pavement. If the materials under the pavement are homogeneous, the electrical resistivity would be considered as the true resistivity 'ρ' ($\Omega \cdot$m) expressed as Equation (1) [7,17]:

$$\rho = \frac{VA}{IL}. \tag{1}$$

The typical electrical resistivities of various types of geomaterials are listed in Table 1. The resistivities exhibit an extensive range from 1 Ω·m for clay to 740,000,000 Ω·m for sandstone [7]. The electrical resistivity of concrete and asphalt depends on the mix proportions because of the influence of the constituent materials (aggregates proportion, content of water and clay, content of ions in water, and pore void, etc.). Therefore, analyzing the correlation between electrical resistivity and constituents of the pavement materials is important in using ERS [1,3,4,6,9,13,14,16,17].

Table 1. Typical electrical resistivity of geomaterials.

Material	Electrical Resistivity (Ω·m)
Granite	300–1,300,000
Sandstone	1–740,000,000
Clay	1–100
Topsoil	250–1700
Gravel	100–1400
Alluvium and sand	10–800
Dry sandy soil	80–1050
Sandy clay/clayey sand	30–215
Sand and gravel	30–225

2.2. Electrode Array and Installation Method

ERS usually requires four electrodes: a positive potential electrode (P+), negative potential electrode (P−), positive electrical current electrode (C+), and negative electrical current electrode (C−). The difference between the two potential electrodes helps in determining the true electrical resistivity. The purpose of ERS is to determine the true electrical resistivity of materials under the pavement. However, as the measured electrical resistance depends on the array of the electrodes, and the actual materials under the pavement are not completely homogeneous, the measured electrical resistivity is considered as the apparent electrical resistivity (ρ_a, Ω·m) [1,5,7,17]. Apparent electrical resistivity can be defined as the equivalent electrical resistance obtained from a heterogeneous medium, which corresponds to the electrical resistance of a homogeneous medium as given in Equation (2):

$$\rho_a = K\frac{V}{I} = KR, \tag{2}$$

where K is a geometric factor.

Usually, the apparent electrical resistivity changes depending on the electrode array because of the change in geometric factor of the heterogeneous materials under the pavement. However, if the materials under the pavement are homogeneous, the measured apparent electrical resistivity can be considered as the true electrical resistivity [3,7,17].

In this study, the dipole–dipole array method (DDAM) was used since DDAM surveys in both vertical and horizontal directions simultaneously for two-dimensional analysis [3,7]. As shown in Figure 2, the survey is performed by increasing the initial spacing a between electrical current electrodes (C+, C−) and potential electrodes (P+, P−) to $2a$, $3a$, ..., na [7]. By increasing the electrode spacing a and n, the effective survey depth increases and the measured electrical resistivity could be related to a specific position in accordance with the electrode spacing [3,8]. The geometric factor (K) is also affected by the electrode spacing as shown in Equation (3):

$$K = n(n+1)(n+2)\pi aR. \tag{3}$$

FEM, which has a wider contact area, is more influenced by contact resistance than PEM [3,8]. In addition, PEM is inefficient since inserting the electrodes into the pavement surface is technically difficult and time-consuming compared with that of FEM. Moreover, the damaged pavement surface caused by electrode insertion could seriously deteriorate in time [3]. However, FEM requires consideration of the contact resistance since the disturbance of the electrical current can increase as the contact area increases; using a wider contact area in FEM can disturb the electrical current more than in PEM [3,8,9].

Therefore, it is necessary to compare the results obtained from both PEM and FEM to determine the applicability of FEM to pavements. In this study, experiments were performed by PEM using 38-mm-long steel nails and by FEM using a hex wrench and a 5-mm-wide copper plate to make the comparison.

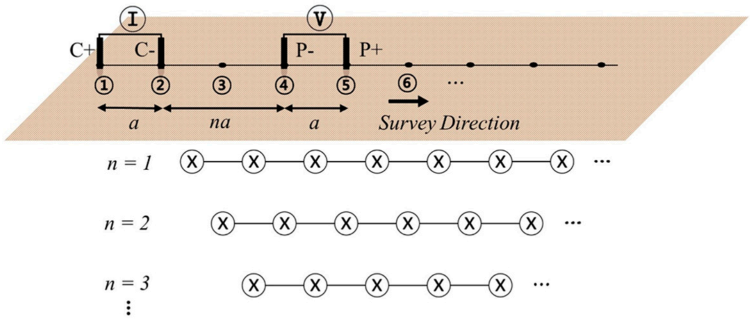

Figure 2. Dipole–dipole array method.

3. Laboratory Experiments

Laboratory experiments were performed using both FEM and PEM to correlate the electrical properties of the pavement materials to the constituent materials analyzed. The results of laboratory experiments will be used as a reference for analyzing the field experiments results. Specimens were prepared in a different size to obtain reliable electrical resistivity data by considering the electrical resistance characteristics of each material as shown in Figure 3.

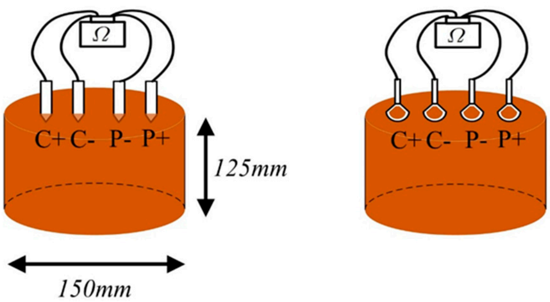

(**a**)

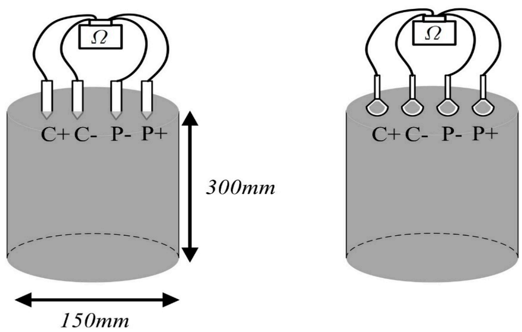

(**b**)

Figure 3. *Cont.*

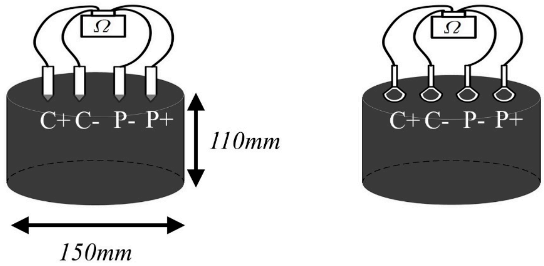

(**c**)

Figure 3. Specimens for laboratory experiments: (**a**) soil material; (**b**) concrete; (**c**) asphalt.

3.1. Soil Specimens

Sieve analysis was carried out to identify the characteristics of the soil materials as shown in Table 2 [18]. The type of field ground soil (nature ground soil), subgrade soil, and subbase soil was classified as poorly graded sand (SP), well-graded sand (SW), and poorly graded gravel (GP), respectively, in accordance with the standard. The compaction curve for each type of soil was generated as shown in Figure 4 [19]. Moreover, the maximum dry unit weight (γ_{dmax}) and optimum water content (ω_{opt}) are summarized in Table 3.

Table 2. Results of sieve analysis.

Type of Soil	Percentage Passing (No. 4 Sieve, %)	Percentage Passing (No. 200 Sieve, %)	Uniformity Coefficient 'Cu'	Coefficient of Curvature 'Cg' (1<, 3>)	Classification
Field ground soil	81.47	2.41	7.43 (>6)	0.825	SP
Subgrade soil	84.10	9.10	13.00 (>6)	1.45	SW
Subbase soil	44.80	2.90	25.00 (>4)	0.35	GP

Table 3. Properties of soils.

Type of Soil	Max. Dry Unit Weight (γ_{dmax}, g/cm^3)	Optimum Water Content (ω_{opt}, %)
Field ground soil	1.99	9.80
Subgrade soil	1.97	9.80
Subbase soil	2.23	6.20

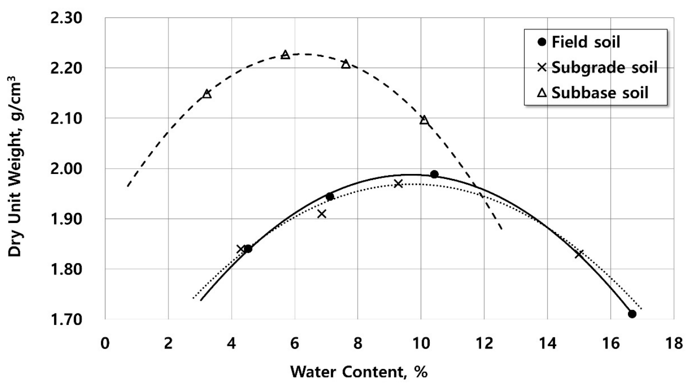

Figure 4. Compaction curve of soil materials.

In many studies, it was indicated that the electrical properties of soil correlate with its constituents and physical property (minerals content, water content, clay content, pore void, etc.) [1,3,4,6,13,14,17]. In particular, water content has the most significant influence on the electrical resistivity of the soil since electrical conductivity is related to the mobility of the ions dissolved in the water that fills the pores of the soil [3,17]. Therefore, four cylindrical specimens (150 mm in diameter and 125 mm in height) with different water content were prepared in order to investigate the effect of water content on the electrical resistivity of the field ground soil, subgrade soil, and subbase soil [19]. The water content of soils used in this study is given in Table 4 [20].

Table 4. Water content of soils (%).

Type of Soil \ Case No.	1	2	3	4
Field ground soil	4.53	7.11	10.42	16.68
Subgrade soil	4.30	6.86	9.28	15.00
Subbase soil	3.22	5.71	7.62	10.10

3.2. Concrete Specimens

The composition of concrete is an important factor influencing the electrical resistivity. In many studies, the effect of w/c on the electrical resistivity of concrete was investigated since the electrical current flows in the concrete by ions dissolved in the pore water [5,8,9]. The w/c is an element of the mix design because it affects the strength and workability of concrete. However, only few research on the effect of fine aggregate modulus (S/a) on the electrical resistivity of concrete has been conducted although it is used in the mix design to control the segregation, slump, and air void [5,8,9,21]. Fine aggregate modulus is the absolute volume ratio of coarse aggregate and fine aggregate in mixture proportion of concrete. Therefore, the effect of S/a on the electrical resistivity of concrete was investigated using PEM and FEM in this study. Cylindrical specimens (150 mm in diameter and 300 mm in height) for three mixture proportions with various S/a [18,22] as indicated in Table 5 were prepared.

Table 5. Mix proportions of concrete.

Case No.	Gmax (mm)	w/c (%)	*S/a* (%)	Unit Quantity (kg/cm^3)			
				Water (W)	Cement (C)	Sand (S)	Gravel (G)
1	25	40.00	38.50	2.41	7.43 (>6)	0.825	SP
2	25	45.00	39.50	9.10	13.00 (>6)	1.45	SW
3	25	50.00	40.50	2.90	25.00 (>4)	0.35	GP

3.3. Asphalt Specimens

In general, electrical conductivity is proportional to the ionic concentration, ionic mobility, viscosity of liquid, and quality of conducting paths determined by textural properties of a material. However, petroleum products (oil, kerosene, gasoline, etc.) are considered as insulators as there is no mobility of ions. Electrical resistivity tends to substantially increase in most cases for petroleum-contaminated soils by exceeding 5,000,000 Ω·m [5,23]. Therefore, asphalt concrete, which consists of aggregate and asphalt binder, could be considered as an insulator with properties of electric insulation, adhesion, and waterproofing [16,23]. In this study, the applicability of ERS to asphalt was investigated by performing PEM and FEM in the laboratory. Cylindrical specimens (150 mm in diameter and 110 mm in height) with different porosities and asphalt content were prepared as indicated in Table 6 [18].

Table 6. Mix proportions of asphalt.

Case No.	1	2
Porosity	4%	10%
Asphalt content	5.8%	5.0%

3.4. Instrumentation of Electrode

Electrode spacing could affect the electrical resistivity of specimens with small sizes (150 mm in diameter). A very small electrode spacing could result in interference between the electrodes, while an extremely wide electrode spacing could result in disturbance of the electrical current field owing to the small space between the electrode and edge of the specimen [5,8]. Therefore, the effect of electrode spacing on the electrical resistivity was investigated by varying the electrode spacing. In this study, six types of electrode spacing were used: (1) a = 20 mm, n = 1 (20-1); (2) a = 20 mm, n = 2 (20-2); (3) a = 20 mm, n = 3 (20-3); (4) a = 30 mm, n = 1 (30-1); (5) a = 30 mm, n = 2 (30-2); (6) a = 40 mm, n = 1 (40-1). Each experiment was repeated five times for each material to improve the reliability of the results. Terrameter SAS 1000 (ABEM, Sundbyberg, Sweden) was used to measure the electrical resistivity for both PEM and FEM.

3.5. Results of Laboratory Experiments

Each electrical resistivity with PEM and FEM was compared graphically and statistically. The correlation was analyzed by paired t-test with significance level of 5% (α = 0.05; α means significance level in statistics). The average values of five repeated experiments were used in the analysis.

3.5.1. Field Ground Soil

The electrical resistivity obtained with both PEM and FEM decreases as the water content increases. However, the electrical resistivity converges to the lowest value when the water content exceeds the optimum water content ω_{opt} (9.80%) in both methods as shown in Figure 5. When the water content is 4.53%, the electrical resistivity through FEM showed significant scattering from 116 Ω·m to 245 Ω·m, compared to the electrical resistivity through PEM from 145 Ω·m to 205 Ω·m. Overall, the average electrical resistivities of the two methods are similar, while there are slight differences in the maximum and minimum electrical resistivities at low water content.

The order of electrical resistivity by electrode spacing using FEM is 20-2, 20-3, 30-1, 20-1, 40-1, and 30-2, while that using PEM is 20-2, 30-1, 20-3, 30-2, 40-1, and 20-1 showing a similar order for the two methods. However, the electrical resistivities using FEM are more scattered than those using PEM at low water content. The electrical resistivity could be disturbed when the pore void in the soil is not sufficiently filled with water and the particle surface is dried. In addition, the loss of adhesion between the soil particles owing to low water content could also cause disturbance of the electrical current [3,14,17]. If the electrical current in FEM, which disperses the electrical current into a wide contact area, flows on the surface of these conditions, it will be more disturbed by the electrical resistance than the PEM, which concentrate the electrical current on the one place. Thus, it is suggested that the disturbance of electrical current at low water content of the field ground soil should be considered in conducting FEM.

In addition to the graphical comparison, statistical analysis was also performed to investigate the applicability of FEM by analyzing the correlation of PEM results with FEM. The paired t-test was used for the analysis by assuming a linear correlation between the results of PEM and FEM [24]. The level of statistical significance was set to α = 0.05 (5% error level). Figure 6 and Table 7 summarize the statistical analysis results. The relationship of the electrical resistivity of the two methods is almost linear and the correlation coefficient (R) is 0.951, indicating a high correlation. In addition, the significance probability (p-value) of 0.091 is also higher than the significance level (0.05), indicating a high correlation between the results of PEM and FEM.

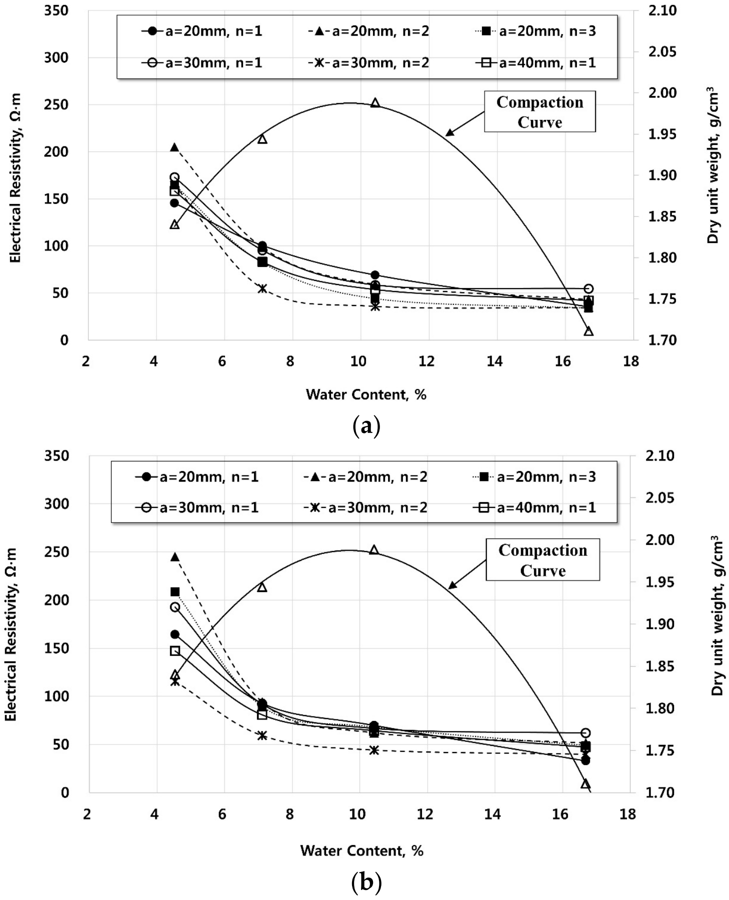

Figure 5. Electrical resistivity of field ground soil using (**a**) PEM and (**b**) FEM.

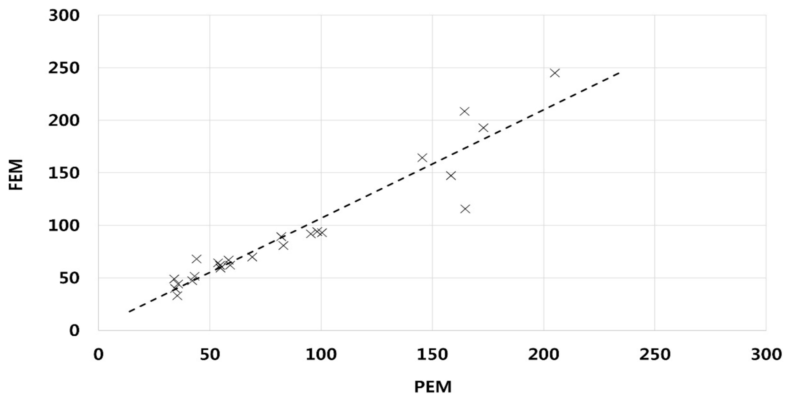

Figure 6. Correlation between electrical resistivity of field ground soil using FEM and PEM.

Table 7. Results of paired *t*-test between PEM and FEM.

Type of Material		Mean (μ)	Standard Deviation (σ)	Standard Error (SE)	*t*-Score	Correlation Coefficient (*R*)	Significance Probability (*p*-Value)
Field ground soil		−6.417	17.832	3.640	−1.763	0.951	0.091
Subgrade soil		−20.042	66.611	13.597	−1.474	0.862	0.154
Subbase soil		−5.125	17.802	3.634	−1.410	0.961	0.172
Concrete	7 days	−5.778	7.175	1.691	−3.417	0.628	0.003
	28 days	−4.556	11.567	2.726	−1.671	0.667	0.113

3.5.2. Subgrade Soil

Similar to the experiment for the field ground soil, four values of water content (4.30%, 6.86%, 9.28%, and 15.00%) were used to investigate its effect on the electrical resistivity of subgrade soil. The electrical resistivity obtained by electrode spacing decreases as the water content increases in both PEM and FEM. When the water content exceeds ω_{opt} (9.80%), the electrical resistivity converges to the lowest value as shown in Figure 7. Although the electrical resistivity of the field ground soil obtained using FEM scatters only at water content of 4.53%, which of the subgrade soil obtained by electrode spacing significantly scatters at two amounts of water content of 4.30% and 6.86% in both PEM and FEM as shown in Figure 7. The scattered electrical resistivity obtained using PEM ranges from 253 Ω·m to 426 Ω·m at 4.30% and from 157 Ω·m to 301 Ω·m at 6.86%, while the scattered electrical resistivity obtained using FEM ranges from 253 Ω·m to 561 Ω·m at 4.30% and from 135 Ω·m to 314 Ω·m at 6.86%. Overall, the minimum electrical resistivities obtained from both methods are similar regardless of the water content, while the maximum value obtained using FEM is larger than that using PEM.

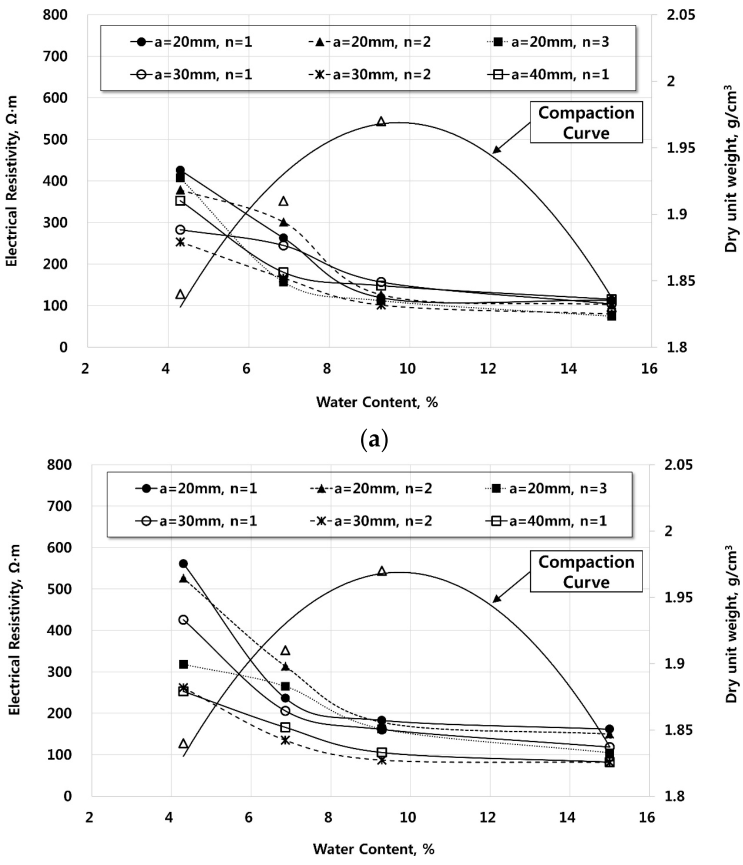

(**b**)

Figure 7. Electrical resistivity of subgrade soil using (**a**) PEM and (**b**) FEM.

The order of electrical resistivity by electrode spacing for PEM is 20-1, 20-3, 20-2, 40-1, 30-1, and 30-2 at 4.30% and 20-2, 20-1, 30-1, 40-1, 30-2, and 20-3 at 6.86% of water content. The order of electrical resistivity using FEM is 20-1, 20-2, 30-1, 20-3, 30-2, and 40-1 at 4.30% and 20-2, 20-3, 20-1, 30-1, 40-1, and 30-2 at 6.86% showing a similar order to PEM. As with the field ground soil, the electrical resistivity using FEM is more scattered than that using PEM because of its larger contact area, causing greater disturbance at low water content.

Statistical analysis was also performed to investigate the correlation between the results of PEM and FEM. The results are summarized in Figure 8 and Table 7. A linear relationship of the electrical resistivities of PEM and FEM is observed and its R value is 0.862, indicating a high correlation. In addition, the p-value of 0.154 is higher than α of 0.05, indicating high correlation between the two methods.

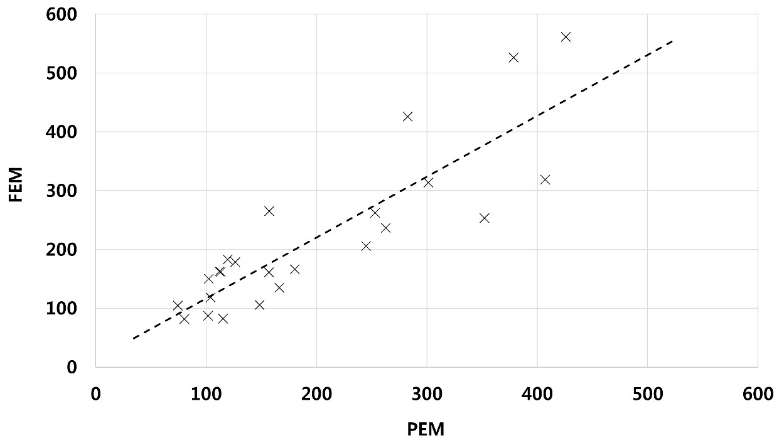

Figure 8. Correlation between electrical resistivity of subgrade soil using FEM and PEM.

3.5.3. Subbase Soil

Similar to the field ground soil and subgrade soil, the effect of water content on the electrical resistivity of subbase soil was investigated by using four values of water content (3.22%, 5.71%, 7.62%, and 10.10%). The electrical resistivity obtained by electrode spacing decreases as the water content increases in both PEM and FEM. When the water content exceeds ω_{opt} (6.20%), the electrical resistivity converges to the lowest value as shown in Figure 9. Based on similar trends observed for the field ground soil, subgrade soil, and subbase soil, it is shown that the electrical resistivity is not affected by water content larger than ω_{opt}, since the adhesion of the soil particles is stabilized by the water content [1,3,17].

The electrical resistivity of subbase soil obtained by electrode spacing significantly scatters in both PEM and FEM when the water content is lower than 3.22%. The scattered electrical resistivity ranges from 90 Ω·m to 228 Ω·m for PEM and 84 Ω·m to 220 Ω·m for FEM as shown in Figure 9. At low water content, since the subbase soil containing large particles of gravel has a smaller adhesion than the other soil, the adhesion between the pole electrode and soil was weakened and the electrical current in PEM was disturbed like FEM. Overall, the electrical resistivities obtained using both methods are similar. The electrical resistivity is high in the order of 20-2, 20-1, 30-1, 20-3, 40-1, and 30-2 in both PEM and FEM showing a small effect of the electrode spacing. The effect of electrode spacing on the electrical resistivity of the subbase soil is similar to that of field ground soil and subgrade soil.

In order to investigate the correlation between PEM and FEM, statistical analysis was also performed. The results are shown in Figure 10 and Table 7. The relationship of the electrical resistivity of the two methods is almost linear and the value of R is 0.961, indicating a high correlation. In addition, the p-value of 0.172 is higher than α of 0.05, which indicates that there is a high correlation between PEM and FEM.

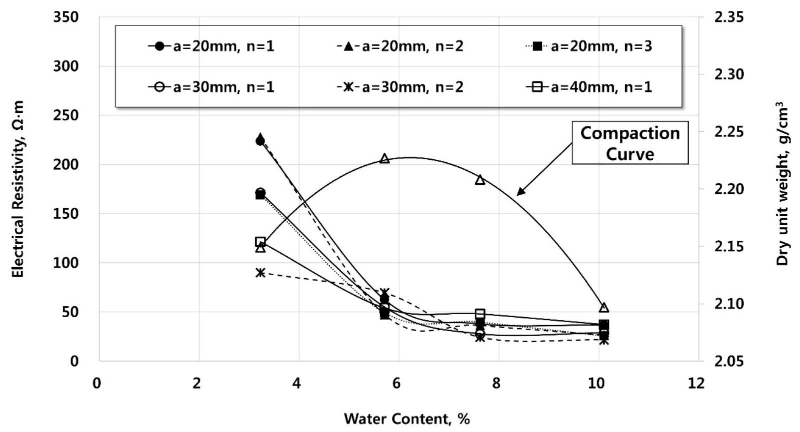

(**a**)

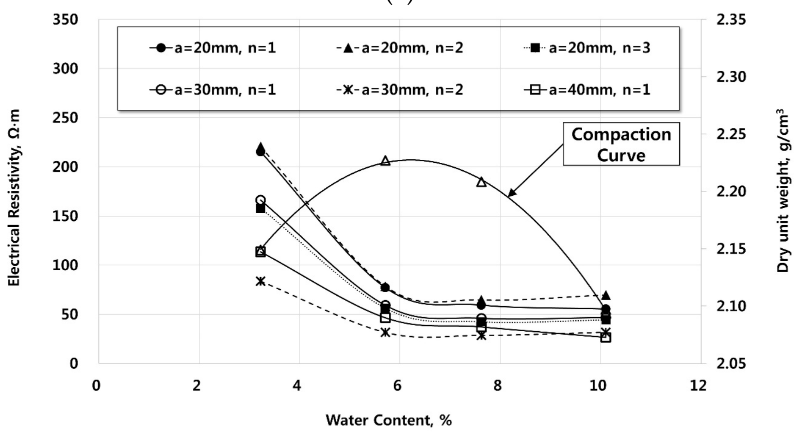

(**b**)

Figure 9. Electrical resistivity of subbase soil using (**a**) PEM and (**b**) FEM.

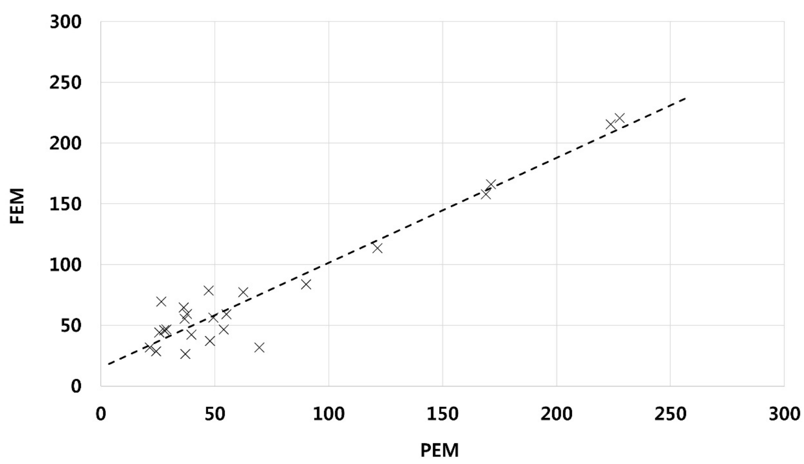

Figure 10. Correlation between electrical resistivity of subbase soil using FEM and PEM.

3.5.4. Concrete

Pore water is the most important factor affecting the electrical resistivity of concrete since the electrical current is transported by the ions dissolved in the pore water. However, the pore water in concrete decreases and the concrete gets dry by generating hydration products and evaporation with increase in curing time [5,9]. To accurately analyze the electrical resistivity of concrete, the effect of curing time should be considered. Therefore, the electrical resistivity of concrete was observed in accordance with the curing time (seven and 28 days).

The effect of S/a (38.50%, 39.50%, and 40.50%) on the electrical resistivity of concrete was investigated. The electrical resistivity increases in accordance with increase of the age of concrete and S/a in both PEM and FEM as shown in Figures 11 and 12. There is a small difference in the electrical resistivity between PEM and FEM. The overall magnitude and variation of the electrical resistivity in accordance with S/a at the age of seven days are smaller than those at the age of 28 days in both PEM and FEM. At the age of seven days, the electrical resistivities obtained using FEM are more scattered than those obtained using PEM in accordance with S/a being influenced by the electrode spacing. The scattered electrical resistivities obtained using FEM range from 16 Ω·m to 32 Ω·m at 38.50%, from 16 Ω·m to 36 Ω·m at 39.50%, and from 18 Ω·m to 46 Ω·m at 40.50% of S/a. On the other hand, at the age of 28 days, the scattering of the electrical resistivity obtained using PEM and FEM is similar in accordance with S/a. This scattering of the electrical resistivity may be caused by the change in chemical activity owing to age, which can affect the electrical current in concrete [5,9].

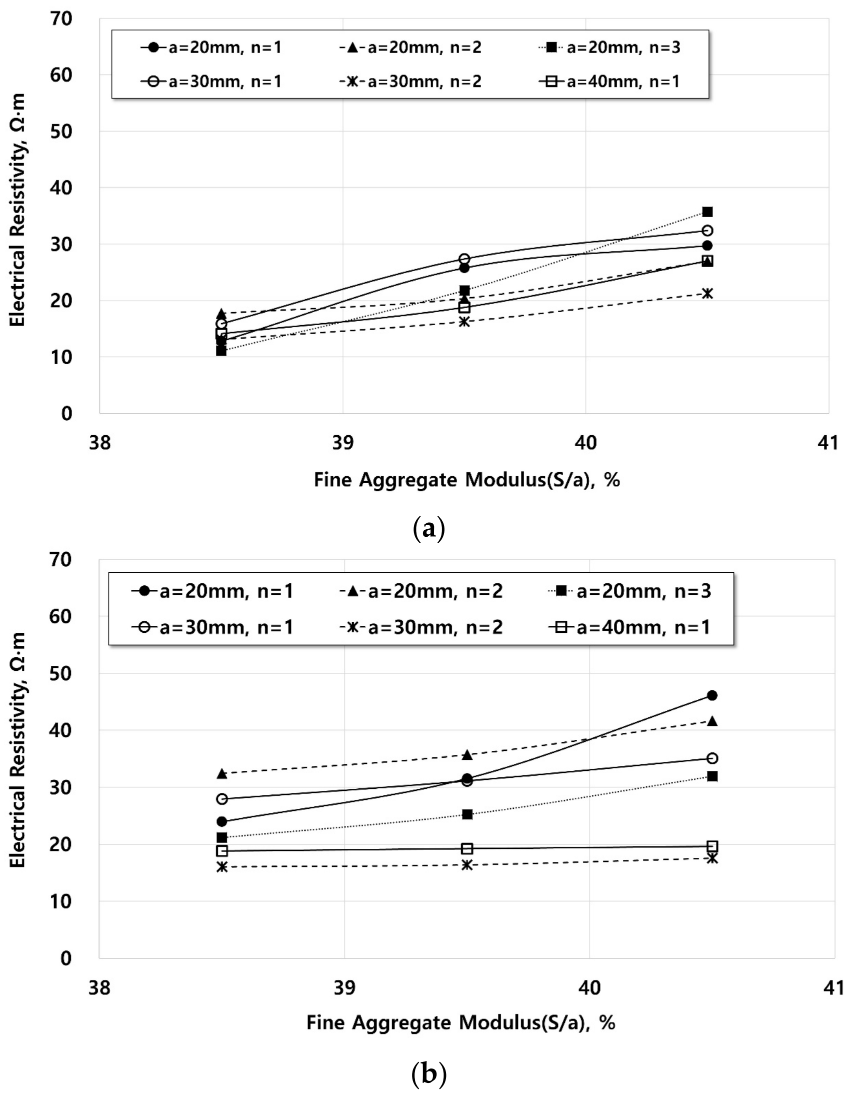

Figure 11. Electrical resistivity of concrete at age of seven days using (**a**) PEM and (**b**) FEM.

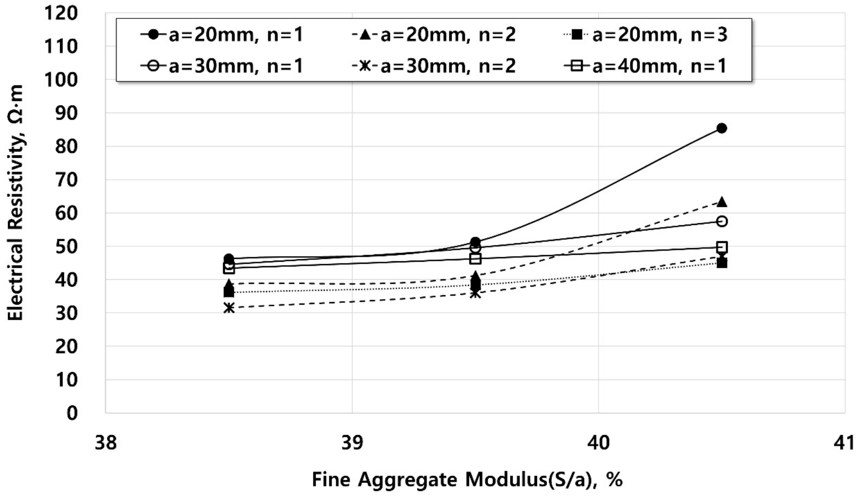

(**a**)

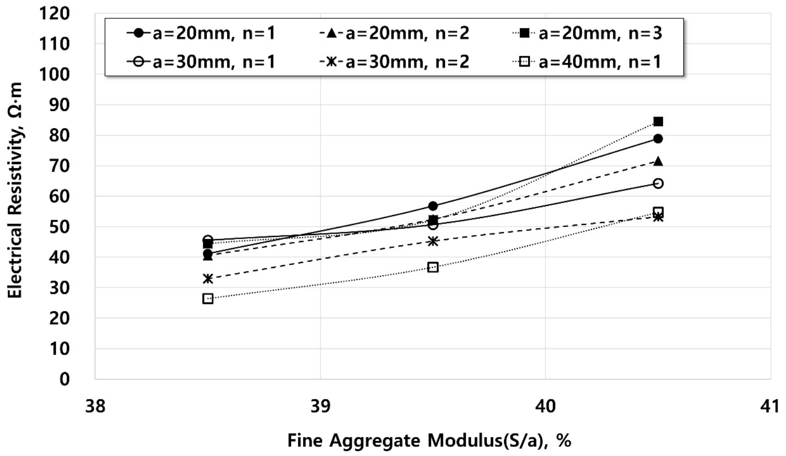

(**b**)

Figure 12. Electrical resistivity of concrete at age of 28 days using (**a**) PEM and (**b**) FEM.

The maximum, minimum, and average electrical resistivities obtained using PEM and FEM at the age of seven and 28 days were compared without considering the electrode spacing. The electrical resistivities of concrete range from 11 Ω·m to 46 Ω·m at the age of seven days and from 26 Ω·m to 85 Ω·m at the age of 28 days within the range of S/a from 38.50% to 40.50%. Although the maximum electrical resistivity of FEM is higher than that of PEM at the age of seven days, there is only a small difference of the electrical resistivity between the two methods in other conditions. Statistical analysis was performed to investigate the correlation between the results of PEM and FEM. The results are summarized in Figure 13 and Table 7. At the age of seven days, the R value of 0.628 is lower than that in soil materials and the p-value of 0.003 is lower than α of 0.05, which indicate low correlation of the electrical resistivity of PEM with that of FEM. At the age of 28 days, although the R value of 0.667 is still lower than that in soil materials, the p-value of 0.113 becomes higher than α of 0.05, showing a more reliable linear relationship.

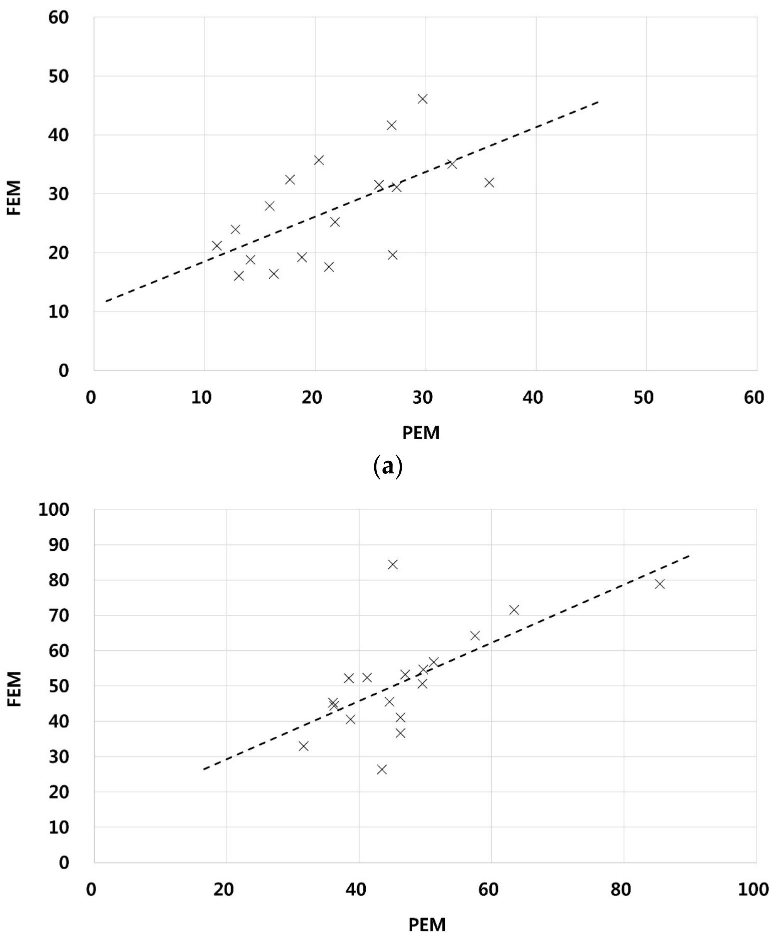

(**a**)

(**b**)

Figure 13. Correlation between electrical resistivity of concrete using FEM and PEM: (**a**) age of seven days; (**b**) age of 28 days.

3.5.5. Asphalt

Since asphalt is an insulator, the measurement of electrical resistivity was carried out after a period of time following salt water spraying to improve the conductivity of the asphalt mixture. Although the salt water was sprayed sufficiently on the surface of the asphalt mixture specimen, a negative resistivity, which should be considered as an error, was measured as shown in Table 8 [16,23,25,26]. Therefore, it is difficult to apply ERS directly to an asphalt surface for investigating the status under the pavement.

Table 8. Electrical resistivity of asphalt mixtures.

Case	Time (min)	1	2	3
1	0	−11.335	−10.241	−11.145
	1	−11.724	−11.263	−10.431
	5	−17.403	−15.807	−14.824
	10	−25.973	−21.984	−20.427
2	0	−2.5342	−2.4916	−2.4114
	1	−2.1127	−2.1991	−2.0087
	5	−2.1127	−2.0446	−1.7849
	10	−2.8714	−2.2917	−3.7613

4. Field Experiments

4.1. Experimental Method

Field experiments were performed to investigate the applicability of FEM for ERS instead of PEM to detect cavities under pavements. As shown in Figure 14, four different cases are simulated in a field site: field ground without cavity, field ground with cavity, concrete pavement without cavity, and concrete pavement with cavity.

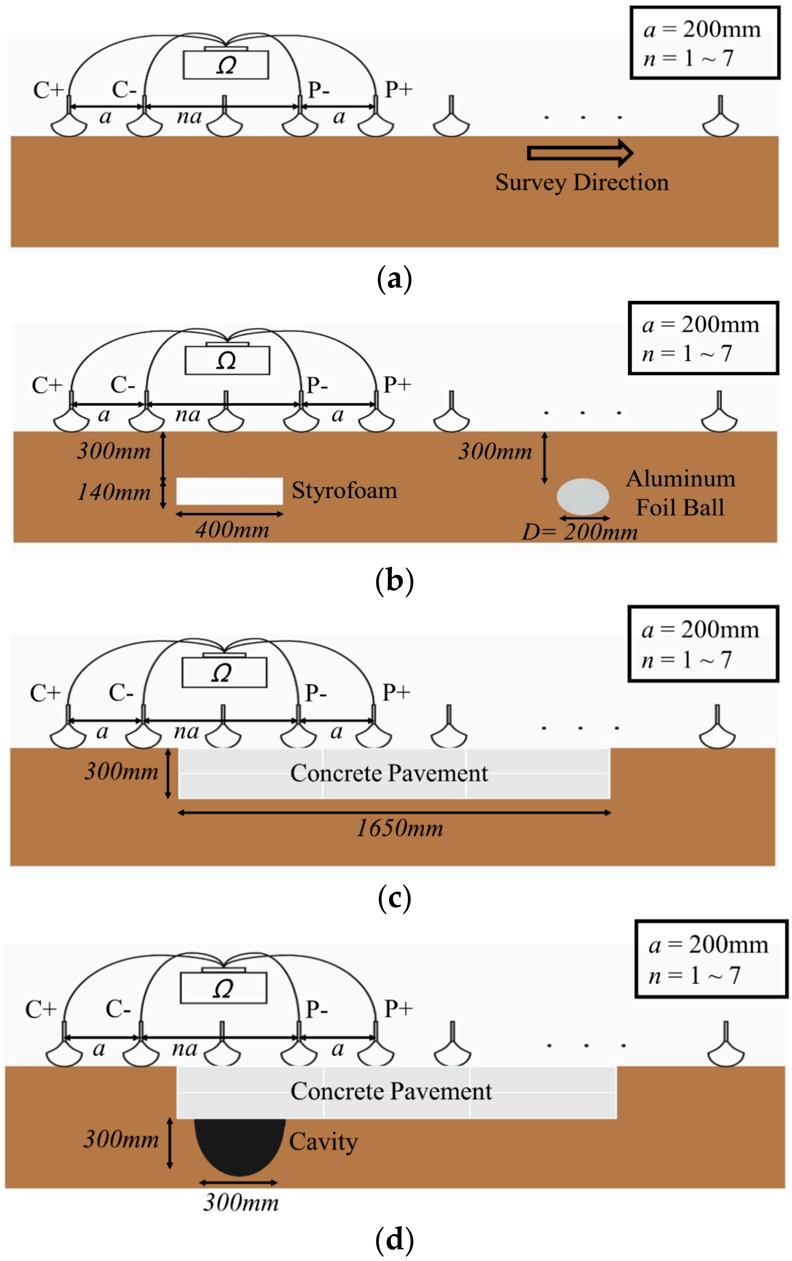

Figure 14. Cases for field experiment: (**a**) field ground without cavity; (**b**) field ground with cavity; (**c**) concrete pavement without cavity; (**d**) concrete pavement with cavity.

To artificially simulate a cavity in the field ground, two types of objects were buried: Styrofoam (400 mm in width, 240 mm in depth, and 140 mm in height) and aluminum foil ball (200 mm in diameter). Generally, the electrical resistivity of a cavity may be substantially high or low depending on the disturbance of electrical current [2,6,13]. Therefore, these objects were used to verify the location of the cavity since Styrofoam is considered as an insulator with an extremely low electrical conductivity, while aluminum foil is considered as a conductor showing a substantially high electrical conductivity. When the cavity was simulated, the excavated area was minimized and carried out natural compaction for a week for minimizing the effect of voids and compaction.

Twelve rectangular concrete specimens (55 mm in width and 15 mm in depth and height) were prepared in accordance with the mix design of Case 1 given in Table 5 to simulate a concrete pavement (1650 mm in width and 300 mm in depth and height) between electrode numbers 12 and 20. A cubic cavity (300 mm in width, depth, and height) was simulated as an empty space under the simulated concrete pavement between electrode numbers 12 and 14.

ERS was carried out using thirty electrodes with a spacing of 200 mm, and $n = 7$: total survey length is 5800 mm in width and 1200 mm in height. The results of ERS were interpreted by DIPRO for Windows V.4.01 (HSGEO, Seongnam, Korea), which is a general-purpose interpretation software. This software inverts the measured electrical resistance into a high-resolution 2D image based on the finite element method as shown in Figures 15–18.

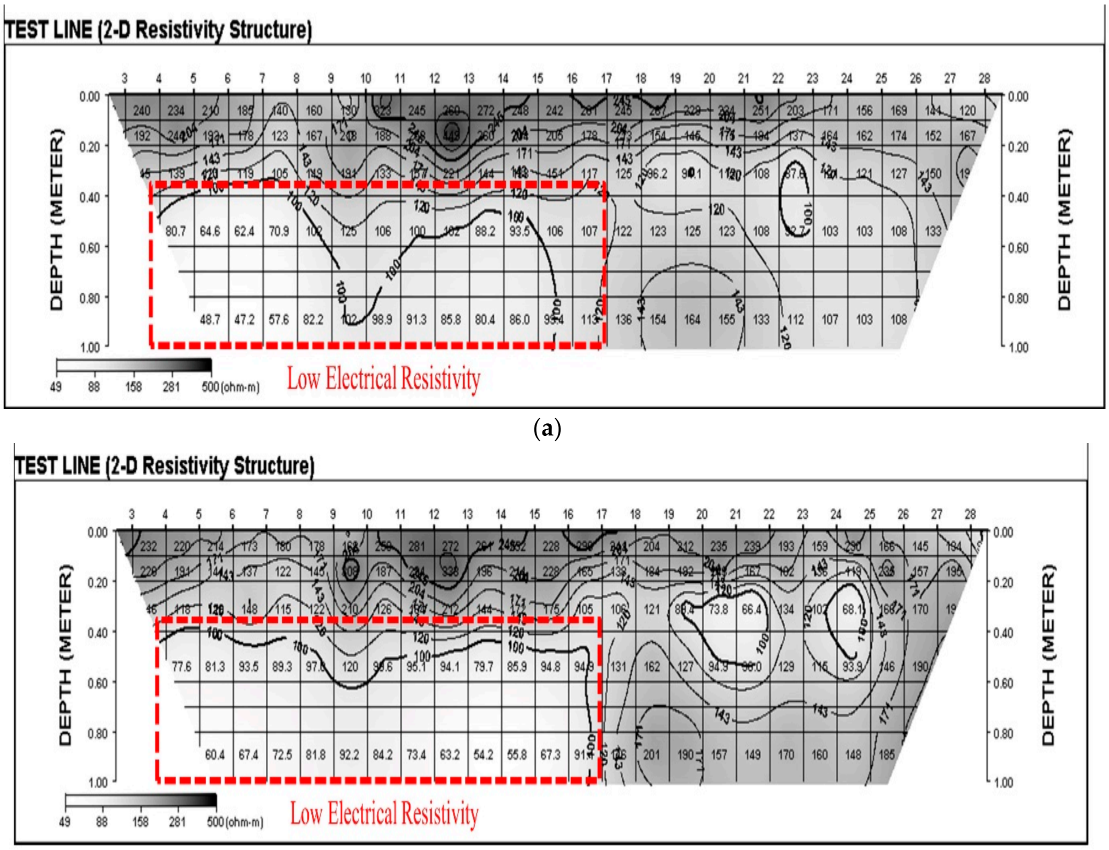

(**a**)

(**b**)

Figure 15. 2D electrical resistivity contour images for field ground without cavity: (**a**) PEM; (**b**) FEM.

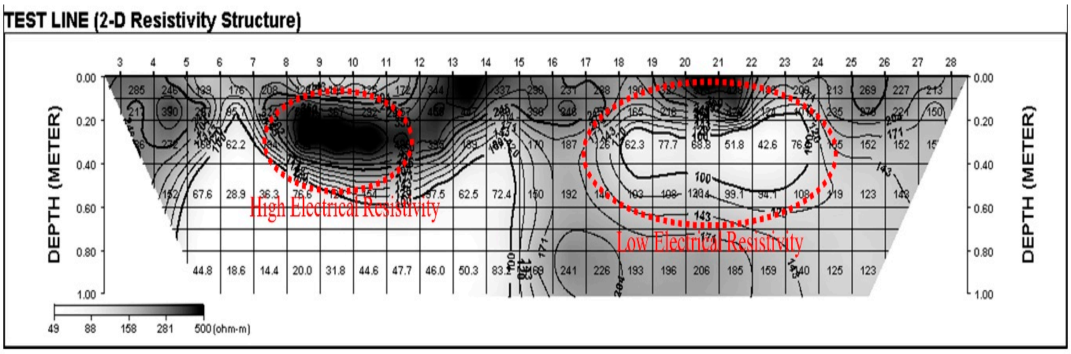

(**a**)

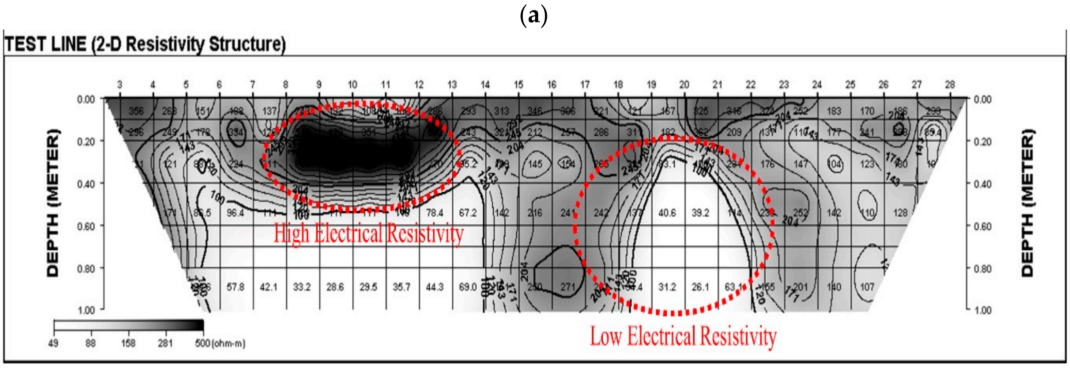

(**b**)

Figure 16. 2D electrical resistivity contour images for field ground with cavity: (**a**) PEM; (**b**) FEM.

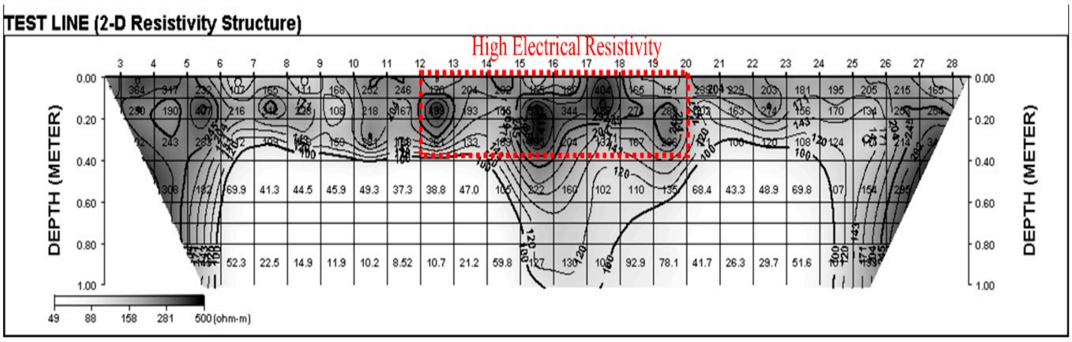

(**a**)

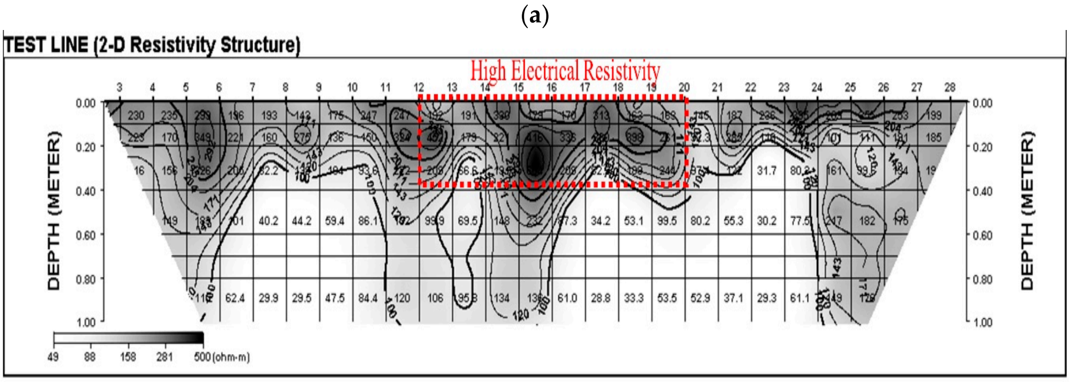

(**b**)

Figure 17. 2D electrical resistivity contour images for concrete pavement without cavity: (**a**) PEM; (**b**) FEM.

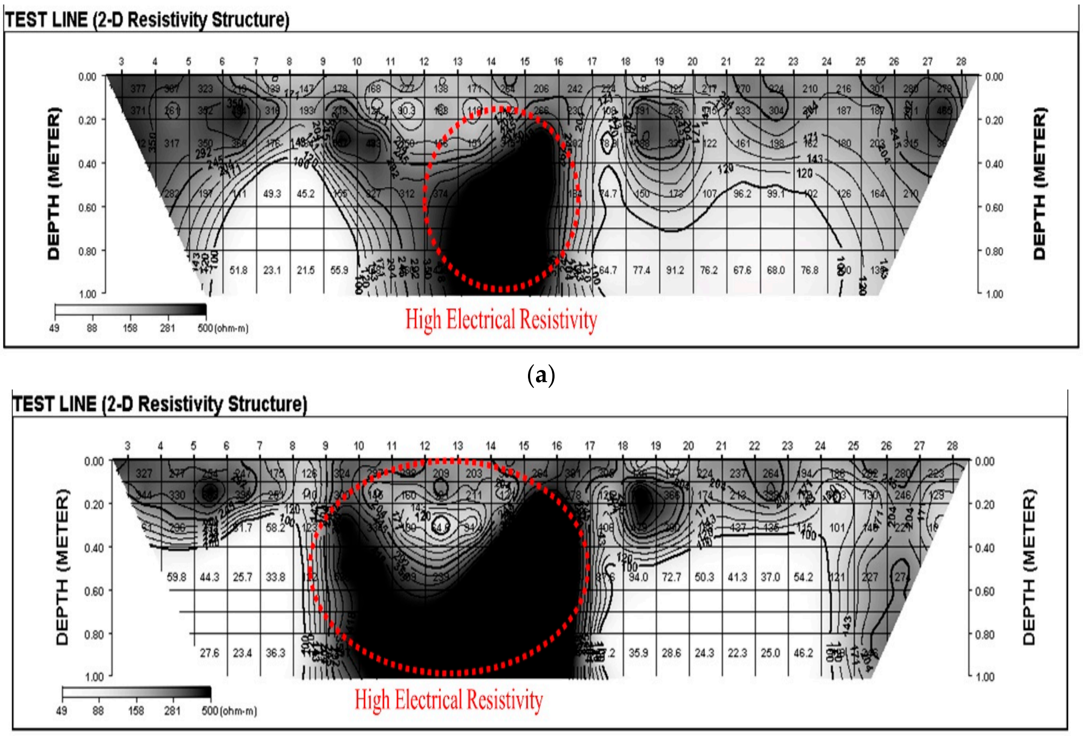

(**a**)

(**b**)

Figure 18. 2D electrical resistivity contour images for concrete pavement with cavity: (**a**) PEM; (**b**) FEM.

4.2. Results of Field Experiments

The results of ERS for the field experiments using PEM and FEM were compared by using the 2D electrical resistivity contour images generated by the software. The analysis of the condition under the pavement according to changes in electrical resistivity (high or low resistivity) was carried out with reference to the laboratory experiments results.

4.2.1. Field Ground without Cavity

PEM and FEM were used as the ERS methods to observe the status in the field ground without any cavity, which will be used as the reference condition for the experiments. Figure 15 shows the 2D electrical resistivity contour images of the field ground without a cavity. The general electrical resistivity of the field ground ranges from 100 Ω·m to 300 Ω·m. Referring to Table 1, the field ground may consist of clay, gravel, or sand materials. Within the dashed box in the figure, the electrical resistivity is below 100 Ω·m, which could mean a high clay and water content. This trend is similar for both PEM and FEM.

4.2.2. Field Ground with Cavity

ERS was carried out to determine whether FEM could be used to detect a cavity existing in a field ground. Figure 16 shows the results of ERS obtained using PEM and FEM. The dashed circle in the figure represents the approximate locations of the Styrofoam and aluminum foil ball buried in the field ground. In general, the electrical resistivity contours obtained using both PEM and FEM are similar to that of the field ground without cavity except for the high and low electrical resistivity locations. A high electrical resistivity between 1000 Ω·m and 2000 Ω·m is observed in both methods at the location where the Styrofoam was buried at 300 mm depth between electrode numbers 9 and 11. It may be associated with the disturbance of the electrical current caused by the Styrofoam with low electrical conductivity. However, a low electrical resistivity is observed in both methods at the location where the aluminum foil ball was buried at 300 mm depth between electrode numbers 20 and 22. The shape of distribution of the low electrical resistivity below 80 Ω·m obtained using PEM is slightly different from that using FEM. The shape of distribution obtained using PEM is horizontally long, while that using FEM is vertically long.

4.2.3. Concrete Pavement without Cavity

The results of ERS performed using PEM and FEM for the concrete pavement without cavity are shown in Figure 17. The dashed box represents the approximate location of the concrete pavement slabs simulated by the rectangular specimens. A high electrical resistivity from 300 Ω·m to 400 Ω·m is observed in both methods at the concrete slab situated between electrode numbers 12 and 20. It may be caused by the effect of the gap between the concrete specimens. However, a low electrical resistivity is observed at the lower location between electrode numbers 6 and 14 and between 16 and 24 in both methods. The appearance of the low electrical resistivity between electrode numbers 6 and 14 is similar to the case of the field ground without cavity, while that between electrode numbers 16 and 24 is different. It may be caused by the ground disturbance during installation of the concrete specimens.

4.2.4. Concrete Pavement with Cavity

ERS was performed to detect the cavity simulated under the concrete pavement using PEM and FEM as shown in Figure 18. The dashed circle represents the approximate location of the cavity. A high electrical resistivity from 1000 Ω·m to 3000 Ω·m is observed at the location of the cavity between electrode numbers 9 and 17 in both methods. However, the shape of the cavity observed using FEM is slightly larger than that obtained using PEM. It may be caused by the effect of the contact resistance on the electrical current owing to the wide contact area of FEM, as PEM uses a point contact by inserting the electrode into the concrete specimen. The wide contact area caused the electrical current to spread widely.

5. Conclusions

The electrical resistivity of soil materials obtained using FEM and PEM in the laboratory decreased as the water content increased. There was little change of the electrical resistivity when the water content exceeded the optimum water content (ω_{opt}). The electrical resistivity by electrode spacing using FEM was significantly more scattered than that using PEM at low water content. However, the scattered electrical resistivity converged to the lowest value as the water content increased. The electrical resistivities in accordance with the electrode spacing for FEM and PEM showed similar trends.

The electrical resistivity of concrete for both methods increased as the fine aggregate modulus (S/a) and curing time increased. However, the electrical resistivity obtained using FEM at the age of seven days significantly scattered differently from PEM. The electrical resistivity obtained at the age of 28 days was not scattered in both methods. Although salt water was sprayed on the surface of the asphalt specimen as an electrolyte, a reasonable electrical resistivity could not be obtained. Statistically, a low correlation between PEM and FEM was observed only for concrete at the age of seven days, while a high correlation between the two methods was observed for other materials (field ground soil, subgrade soil, subbase soil, and concrete at the age of 28 days).

In the field experiments, a high electrical resistivity was observed for the cavity simulated by the Styrofoam or empty space, while a low electrical resistivity was observed for the aluminum foil ball. The distribution of the high or low electrical resistivity in the 2D contour caused by the Styrofoam, empty space, and aluminum foil ball obtained using FEM was wider than that using PEM. However, the results using both methods exactly predicted the actual location of the cavity simulated in the ground and under the pavement.

Based on the results, it is shown that using FEM for ERS instead of PEM is acceptable as the difference in the results between the two methods is small. In addition, FEM is more advantageous since it is easier to use and causes less damage to the pavement surface compared with PEM.

Acknowledgments: This research was supported by a research grant of INHA University and by the Basic Science Research Program of the National Research Foundation (NRF) of Korea funded by the Korean Ministry of Education (NRF-2014R1A1A2055003).

Author Contributions: Regarding the author's participation in this research, Chang-Seon Park planned and performed the laboratory and field experimental tests. He also drafted the manuscripts. Jin-Hoon Jeong and Hae-Won Park performed field and laboratory tests and also analyzed experiments. Kyoungchul Kim guided this study, provided valuable comments and revised it.

Conflicts of Interest: The authors declare no conflict of interest.

References

1. Kalinski, R.J.; Kelly, W.E. Electrical-Resistivity Measurements for Evaluating Compacted-Soil Liners. *J. Geotech. Eng.* **1994**, *120*, 451–457. [CrossRef]
2. Louis, I.F.; Louis, F.I.; Bastou, M. Accurate Subsurface Characterization for Highway Applications Using Resistivity Inversion Methods. *J. Electr. Electron. Eng.* **2002**, 43–55.
3. Samouëlian, A.; Cousin, I.; Tabbagh, A.; Bruand, A.; Richard, G. Electrical Resistivity Survey in Soil Science: A Review. *Soil Tillage Res.* **2005**, *83*, 173–193. [CrossRef]
4. Park, S.G.; Kim, C.R.; Son, J.S.; Kim, J.H.; Yi, M.J.; Cho, S.J. Detection of Lime Silicate Cavities by 3-D Resistivity Survey. *Econ. Environ. Geol.* **2006**, *39*, 597–605.
5. Farooq, M.; Park, S.G.; Song, Y.S.; Kim, J.H. Mortar Characterization using Electrical Resistivity Method. *Geophys. Geophys. Explor.* **2009**, *12*, 215–220.
6. Gambetta, M.; Armadillo, E.; Carmisciano, C.; Stefanelli, P.; Cocchi, L.; Caratori Tontini, F. Determining Geophysical Properties of a Nearsurface Cave through Integrated Microgravity Vertical Gradient and Electrical Resistivity Tomography Measurements. *J. Cave Karst Stud.* **2010**, *73*, 11–15. [CrossRef]
7. Reynolds, J.M. *An Introduction to Applied and Environmental Geophysics*; John Wiley & Sons: New York, NY, USA, 2011; ISBN 978-1-11-995714-0.
8. Millard, S.G. Reinforced Concrete Resistivity Measurement Techniques. *Proc. Inst. Civ. Eng.* **1991**, *91*, 71–88. [CrossRef]
9. Polder, R.B. Test Methods for on Site Measurement of Resistivity of Concrete—A RILEM TC-154 Technical Recommendation. *Constr. Build. Mater.* **2001**, *15*, 125–131. [CrossRef]
10. Park, J.-Y.; Sohn, D.-S.; Lee, J.-H.; Jeong, J.-H. A Study on Joint Position at Concrete Pavement with Box Culverts. *Int. J. Highw. Eng.* **2012**, *14*, 45–53. [CrossRef]
11. Yeom, W.S.; Jeong, H.S.; Yan, Y.; Sohn, D.S.; Lee, J.H.; Jeong, J.H. Optimal Joint Position in Concrete Pavement Slab over Skewed Box Culvert. *Int. J. Highw. Eng.* **2013**, *15*, 47–55. [CrossRef]
12. Sohn, D.S.; Lee, J.H.; Jeong, H.S.; Park, J.Y.; Jeong, J.H. A Method for Evaluation of Hollow Existence in Sublayers of Concrete Pavement Considering Pavement Stiffness. *Int. J. Highw. Eng.* **2013**, *15*, 95–102. [CrossRef]
13. Kim, J.-H.; Hong, W.-P.; Kim, G.-B. Interpretation of Soft Ground Deformation under Embankment using the Electrical Resistivity Survey. *J. Eng. Geol.* **2011**, *21*, 117–124. [CrossRef]
14. Cai, G.H.; Du, Y.J.; Liu, S.Y.; Singh, D.N. Physical Properties, Electrical Resistivity, and Strength Characteristics of Carbonated Silty Soil Admixed with Reactive Magnesia. *Can. Geotech. J.* **2015**, *52*, 1699–1713. [CrossRef]
15. Sentenac, P.; Hogson, T.; Keenan, H.; Kulessa, B. Small Scale Monitoring of a Bioremediation Barrier Using Miniature Electrical Resistivity Tomography. *J. Appl. Geophys.* **2015**, *115*, 24–31. [CrossRef]
16. Pan, P.; Wu, S.; Xiao, F.; Pang, L.; Xiao, Y. Conductive Asphalt Concrete: A Review on Structure Design, Performance, and Practical Applications. *J. Intell. Mater. Syst. Struct.* **2015**, *26*, 755–769. [CrossRef]
17. Park, S.G.; Kim, J.H.; Cho, S.J.; Yi, M.J.; Son, J.S. Electrical Resistivity Characteristic of Soils. *Geophys. Geophys. Explor.* **2004**, 847–854.
18. MLTMA (Ministry of Land, Transport and Maritime Affairs). *Standard Specification of Road Construction*; Ministry of Land, Transport and Maritime Affairs: Sejong City, Korea, 2009.
19. ASTM D698-12e2. *Standard Test Methods for Laboratory Compaction Characteristics of Soil Using Standard Effort (12,400 ft-lbf/ft^3 (600 kN-m/m^3))*; ASTM International: West Conshohocken, PA, USA, 2012. [CrossRef]
20. ASTM D2216-10. *Standard Test Methods for Laboratory Determination of Water (Moisture) Content of Soil and Rock by Mass*; ASTM International: West Conshohocken, PA, USA, 2010. [CrossRef]

21. Han, C.-G.; Han, I.-D. Quality of High-strength Concrete depending on Various S/A and Unit Water Contents. *J. Archit. Inst. Korea Struct. Constr.* **2015**, *31*, 35–42. [CrossRef]
22. ASTM C192/C192M-16a. *Standard Practice for Making and Curing Concrete Test Specimens in the Laboratory*; ASTM International: West Conshohocken, PA, USA, 2016. [CrossRef]
23. Delaney, A.J.; Peapples, P.R.; Arcone, S.A. Electrical Resistivity of Frozen and Petroleum-contaminated Fine-grained Soil. *Cold Reg. Sci. Technol.* **2001**, *32*, 107–119. [CrossRef]
24. Bhatt, S.; Jain, P.K. Correlation between Electrical Resistivity and Water Content of Sand—A Statistical Approach. *Am. Int. J. Res. Sci. Technol. Eng. Math.* **2014**, *6*, 115–121.
25. Cho, I.K.; Kim, J.H.; Chung, S.H.; Suh, J.H. Negative Apparent Resistivity in Resistivity Method. *Geophys. Geophys. Explor.* **2002**, *5*, 199–205.
26. Jung, H.; Min, D.; Lee, H.; Oh, S.; Chung, H. Negative Apparent Resistivity in Dipole–dipole Electrical Surveys. *Explor. Geophys.* **2009**, *40*, 33–40. [CrossRef]